BMB Reports - Manuscript Submission

Manuscript Draft

Manuscript Number: BMB-21-142

Title: MiR-141-3p regulates myogenic differentiation in C2C12 myoblasts via CFL2-YAP-mediated mechanotransduction.

Article Type: Article

Keywords: miR-141-3p; CFL2; Mechanotransduction; Differentiation; Myogenesis

Corresponding Author: Wan Lee

Authors: Mai Thi[1], Wan Lee[1,*]

Institution: [1]Department of Biochemistry, Dongguk University College of Medicine,

MiR-141-3p regulates myogenic differentiation in C2C12 myoblasts via CFL2-YAP-mediated mechanotransduction.

Mai Thi Nguyen and Wan Lee[#]

Department of Biochemistry, Dongguk University College of Medicine, 123 Dongdae-ro, Gyeongju 38066, Republic of Korea

[#] **Corresponding author:** Wan Lee,
Department of Biochemistry, Dongguk University College of Medicine, 123 Dongdae-ro, Gyeongju 38066, Republic of Korea. Tel: +82.54-770-2409, Fax: +82.54-770-2447, Email: wanlee@dongguk.ac.kr

ABSTRACT

Skeletal myogenesis is essential to keep muscle mass and integrity, and impaired myogenesis is closely related to the etiology of muscle wasting. Recently, miR-141-3p has been shown to be induced under various conditions associated with muscle wasting, such as aging, oxidative stress, and mitochondrial dysfunction. However, the functional significance and mechanism of miR-141-3p in myogenic differentiation have not been explored to date. In this study, we investigated the roles of miR-141-3p on CFL2 expression, proliferation, and myogenic differentiation in C2C12 myoblasts. MiR-141-3p appeared to target the 3'UTR of *CFL2* directly and suppressed the expression of CFL2, an essential factor for actin filament (F-actin) dynamics. Transfection of miR-141-3p mimic in myoblasts increased F-actin formation and augmented nuclear Yes-associated protein (YAP), a key component of mechanotransduction. Furthermore, miR-141-3p mimic increased myoblast proliferation and promoted cell cycle progression throughout the S and G2/M phases. Consequently, miR-141-3p mimic led to significant suppressions of myogenic factors expression, such as MyoD, MyoG, and MyHC, and hindered the myogenic differentiation of myoblasts. Thus, this study reveals the crucial role of miR-141-3p in myogenic differentiation via CFL2-YAP-mediated mechanotransduction and provides implications of miRNA-mediated myogenic regulation in skeletal muscle homeostasis.

Key Words: miR-141-3p; CFL2; mechanotransduction; differentiation; myogenesis

1. INTRODUCTION

Skeletal muscle is a dynamic and plastic tissue essential for proper locomotion and metabolic functioning (1). Muscle wasting or atrophy is closely linked to various conditions associated with the inhibition of myogenesis, such as senescence, ER stress, oxidative stress, and mitochondrial dysfunction (2). Myogenesis is a well-coordinated complex process and underlies myofiber formation for muscle development and regeneration (3). During myogenesis, satellite cells exit quiescence, rapidly proliferate until they exit the cell cycle, and then after the activations of myogenic factors, differentiate into myotubes (3). Over the past two decades, numerous studies have shown the implication of miRNAs in muscle homeostasis and myogenesis (4). However, the mechanisms whereby specific miRNAs regulate myogenic differentiation remain elucidated.

MicroRNAs (miRNAs) comprise endogenous short non-coding RNAs that suppress gene expressions through binding to their 3'UTRs of target mRNAs (5). Accumulating evidence has suggested that miRNAs are critical modulators of skeletal muscle proliferation, differentiation, and regeneration (6). MiR-141-3p, a member of miR-200 family, is proposed as an oncogenic miRNA because it facilitates tumorigenesis, metastasis, and resistance to chemotherapy by promoting cell proliferation, growth, and survival (7, 8). Interestingly, miR-141-3p is upregulated during various conditions related to muscle wasting, including ER stress, oxidative stress, and mitochondrial dysfunction (9-11). Moreover, miRNA-141-3p expression was

47 also increased in various cells during cellular senescence, which is associated with sarcopenia (9, 12, 13).
48 In this respect, miR-141-3p may be implicated in myogenesis and muscle homeostasis by regulating cell
49 proliferation and growth. However, the significance of miR-141-3p in myogenic progenitor cells have not
50 been explored.

51 Based on the results of *in silico* miR-target prediction analysis, Cofilin 2 (CFL2) is suggested as a
52 tentative target of miR-141-3p. CFL2 is a skeletal muscle-specific actin-depolymerizing factor protein,
53 which promotes the disassembly of filamentous actin (F-actin) (14). Many studies suggest that CFL2 is
54 essential for the maintenance of skeletal muscle architecture through regulating actin cytoskeleton
55 rearrangement (14). CFL2 knockout caused lethality in mice within seven days of birth due to skeletal
56 muscle weakness, sarcomere structure disruption, and F-actin accumulations (15). Furthermore, CFL2
57 knockout developed degenerative myopathy with thin muscle fiber, protein aggregates, and abnormal
58 mitochondria (16). We recently revealed that the knockdown of CFL2 promoted cell proliferation and
59 inhibited myoblast differentiation (17). Other investigations have suggested that CFL-mediated actin
60 cytoskeleton rearrangement regulates myoblast proliferation and differentiation (18, 19). Although prior
61 research has shown the indispensable roles of CFL2 in myogenesis, little is known about the miRNAs that
62 regulate CFL2 and their significance in myogenic differentiation.

Here, we demonstrated the critical role of miR-141-3p on CFL2 expression and myogenic differentiation. Interestingly, miR-141-3p hindered CFL2 expression by targeting *CFL2* 3'UTR directly. Moreover, we showed how miR-141-3p modulated myoblast proliferation, myogenic factor expression, and differentiation in conjunction with mechanotransduction. Thus, our study suggests that miR-141-3p plays an important part in myogenesis via the CFL2/F-actin/YAP axis and provided implications of miRNA-mediated actin dynamics as a myogenic regulatory mechanism.

2. RESULTS

2.1. MiR-141-3p targeted *CFL2*.

We hypothesized that miR-141-3p might inhibit myoblast differentiation by suppressing CFL2. Therefore, we first investigated whether miR-141-3p suppresses CFL2 expression in myoblasts. According to miRWalk and TargetScan analysis, CFL2 is a putative target of miR-141-3p due to a miR-141-3p binding site on the *CFL2* 3´UTR (Fig. 1A). To determine the binding between miR-141-3p and *CFL2* 3'UTR, the *CFL2* 3'UTR segment containing a tentative binding site for miR-141-3p (wild-type; CFL2-*wt*) or mutated sequences (CFL2-*mut*) were constructed (Fig. 1B) and then cloned into the pmirGLO vector. As shown in Fig. 1C, co-transfection with miR-141-3p mimic and wild-type (CFL2-*wt*) decreased luciferase activity as compared with scRNA. In contrast, mutations in a tentative binding site (CFL2-*mut*) entirely abrogated the suppressive effect of miR-141-3p in CFL2-*wt*, confirming direct binding of miR-141-3p to *CFL2* 3'UTR. Next, this study examined whether miR-141-3p suppresses CFL2 expression in myoblasts. The cells transfected with miR-141-3p mimic exhibited a reduction of CFL2 protein expression (Fig. 1D). Moreover, the transcription of CFL2 was also suppressed slightly but significantly by miR-141-3p mimic (Fig. 1E). These results indicate that miR-141-3p regulates CFL2 expression by directly targeting *CFL2* 3'UTR.

2.2. MiR-141-3p augmented F-actin and nuclear YAP.

Since we previously reported that CFL2 knockdown in myoblasts caused a marked accumulation of F-actin (17), we next determined whether miR-141-3p could modulate the reorganization of F-actin. Although transfection with CFL2 siRNAs, namely siCFL2(1) and siCFL2(2), reduced CFL2 protein levels by ~55% (Fig. 2A), we found that siCFL2(2) had a slight cytotoxic effect at a dose of 200 nM. Therefore, we used siCFL2(1) for the subsequent experiments. Transfection with miR-141-3p mimic in myoblasts markedly increased miR-141-3p level (>200-fold, data not shown). Remarkably, miR-141-3p or siCFL2 caused F-actin accumulation (Fig. 2B). Given that the total amount of actin remained constant during the differentiation period in all groups, these F-actin increases appeared to be the consequence of impaired F-actin depolymerization. Thus, it indicated that miR-141-3p restricts actin dynamics and augments F-actin by suppressing CFL2 in myoblasts. F-actin has been shown to stimulate the nuclear translocation of transcriptional coactivator YAP, which modulates mechanotransduction in the Hippo signaling pathway and activates proliferative transcriptional programs (20). To investigate the function of miR-141-3p on YAP expression and translocation, we next determined the phosphorylation and localization of YAP. Transfection of miR-141-3p mimic dramatically reduced the phosphorylation of YAP in the cytoplasm and subsequently allowed YAP to translocate into the nucleus (Figs. 2C and D). Thus, it appeared that the effect of miR-141-3p on the cytoplasmic/nuclear redistribution of YAP was mainly ascribed to CFL2 suppression.

2.3. MiR-141-3p promoted myoblast proliferation.

Since CFL2 deficiency was previously shown to hinder myogenic differentiation by promoting cell proliferation (17), the effect of miR-141-3p on proliferation and cell cycle was examined in myoblasts. EdU incorporation analysis showed that siCFL2 significantly increased the proportion of EdU-positive myoblasts (Figs. 3A and B), which demonstrated CFL2 depletion promoted myoblast proliferation. As expected, miR-141-3p mimic also drastically increased EdU-positive myoblasts, while co-transfection with antimiR-141 rescued EdU incorporation similar to those observed after scRNA transfection (Figs. 3A and B), suggesting that miR-141-3p could promote myoblast proliferation. Next, we analyzed the transcriptions of PCNA and CCND1, which are YAP target genes associated with cell cycle progression and cell proliferation. According to *q*RT-PCR, the transcript levels of PCNA and CCND1 in myoblasts were induced significantly by miR-141-3p mimic (Fig. 3C). Furthermore, we determined the effect of miR-141-3p on cell cycle phases based on flow cytometry. The transfection of miR-141-3p mimic decreased the number of G0/G1-phase cells but increased the number of S- and G2/M-phase cells (Fig. 3D). Thus, an increase of miR-141-3p in myoblasts was found to promote cell proliferation and cell cycle progression.

2.4. MiR-141-3p inhibited myogenic factors expressions.

To investigate whether miR-141-3p modulates myogenic factors expression in myoblasts, C2C12 cells were differentiated for three days after transfection with scRNA, siCFL2, miR-141-3p mimic, or antimiR-141-3p, and then the protein expressions of myogenic factors were analyzed (Figs. 4 and B).

Transfection of siCFL2 suppressed CFL2 expression by about 55% versus scRNA and drastically reduced the protein expression of myogenic factors, such as MyoD and MyoG. Similarly, miR-141-3p mimic transfection inhibited the protein expression of CFL2 markedly and reduced myogenic factors' levels compared with scRNA controls. Furthermore, the co-transfection of miR-141-3p and antimiR-141 rescued myogenic factor levels similar to scRNA transfection (Figs. 4A and B). The ineffectiveness of antimiR-141 alone may be ascribed to the low level of endogenous miR-141-3p and the abundance of CFL2 in C2C12 myoblasts. Because CFL2 knockdown inhibits myogenic differentiation and there are no putative miR-141-3p seed binding sequences on the 3'UTRs of MyoD, MyoG, and MyHC, the suppression of theses factors by miR-141-3p mimic is attributed to CFL2 reduction. Thus, it is suggested that miR-141-3p plays a critical role in the regulation of myogenic factors in myoblasts.

2.5. MiR-141-3p hindered myoblast differentiation.

Since miR-141-3p suppressed myogenic factors expression, we examined the effect of miR-141-3p on myoblast differentiation. C2C12 myoblasts were differentiated for five days after transfection with scRNA, siCFL2, miR-141-3p mimic, or antimiR-141-3p. The differentiation of myoblasts was determined quantitatively by immunocytochemistry, as shown in Figs. 4C and D. The knockdown of CFL2 dramatically inhibited myotube formation. In addition, the percentage area of MyHC-positive cells, differentiation indices, fusion indices, and myotube widths indicated that CFL2 downregulation resulted in impaired

myogenic differentiation (Figs. 4C and D). Similarly, transfection of miR-141-3p mimic inhibited myoblast differentiation as assessed by cytochemistry. Furthermore, co-transfection with antimiR-141-3p completely abolished the inhibitions of myogenic differentiation and myotube formation mediated by miR-141-3p mimic (Figs. 4C and D). Collectively, these results suggest that miR-141-3p hinders myogenic factors expression and differentiation.

3. DISCUSSION

MiRNAs have been implicated in myogenesis and muscle homeostasis by variously regulating proliferation, the cell cycle, and differentiation (6). In this study, we unveiled the crucial roles of miR-141-3p on CFL2 expression, myoblast proliferation, and differentiation. The following highlights the key contributions of our study; (i) MiR-141-3p suppressed CFL2 expression by directly targeting the *CFL2* 3'UTR. (ii) Transfection with miR-141-3p mimic augmented F-actin and increased nuclear YAP in myoblasts. (iii) MiR-141-3p mimic increased proliferation and promoted cell cycle progression of myoblasts. (iv) MiR-141-3p mimic markedly suppressed the levels of myogenic factors and hindered differentiation of myoblasts.

Hsa-miR-141-3p belongs to the miR-200 family consists of five miRNAs viz miR-141, 200a, 200b, 200c, and 429 in vertebrates (8). Although the biological importance of miR-141-3p in myogenesis has never been explored, it has been found to be induced in a range of muscle wasting disorders, including oxidative stress (10), mitochondrial dysfunction (11), and senescence (9, 12, 13). Hence, we hypothesize that dysregulation of miR-141-3p contributes substantially to impaired myogenesis and muscle wasting. Notably, we found miR-141-3p mimic stimulated myoblast proliferation in myoblasts and subsequently suppressed myogenic differentiation (Figs. 3 and 4). Proliferation and differentiation of myoblasts have long been established to be inversely associated during myogenesis, and thus, arrest in proliferation is a

158 prerequisite of myogenic differentiation (3). In this aspect, the promotion of proliferation by miR-141-3p
159 is intimately connected to the impaired myogenic differentiation in myoblasts. Recent research on various
160 cancers has supported the roles of miR-141-3p on the cell cycle, apoptosis, and proliferation. MiR-141-3p
161 was upregulated in various malignancies, such as colon, lung, prostate, and cervical cancers (7). In addition,
162 overexpression of miR-141-3p caused cell proliferation, while knockdown of miR-141-3p suppressed the
163 proliferation of various cells (21-24). This study showed that miR-141-3p stimulated the gene expression
164 of PCNA and CCND1, which are target genes of YAP and related to cell cycle progression. This result is
165 in line with previous reports that miR-141-3p elevated PCNA in the intestine of mice (25) and CCND1 in
166 nasopharyngeal carcinoma (26). Therefore, the role played by miR-141-3p on myoblast differentiation may
167 be primarily ascribed to increased proliferation and cell cycle progression in myoblasts.

168 Then what is the underlying molecular mechanism whereby miR-141-3p promotes myoblast
169 proliferation? It should be highlighted that miR-141-3p mimic transfection directly suppressed CFL2
170 expression and increased F-actin in myoblasts (Fig. 2). CFL2 regulates actin remodeling by cleaving F-
171 actin and thus, plays an essential role in cytoskeleton dynamics (19). Interestingly, actin dynamics is
172 suggested as a key regulator of YAP activation in the Hippo signaling pathway (27). Previously, F-actin
173 was reported to inhibit YAP/TAZ phosphorylation, which increases YAP activation and cell proliferation
174 as a mechanotransduction mechanism (20). Furthermore, F-actin depolymerizing proteins, including CFL

and Gelosin, inactivates the Hippo signaling by increasing YAP and TAZ phosphorylations [16]. Thus, CFL-mediated actin remodeling is closely linked to the mechanotransduction-induced nuclear translocation of YAP and cell proliferation (18, 19). Our previous study showed that CFL2 knockdown augmented F-actin formation, enhanced cell cycle progression, and stimulated myoblast proliferation (17). Similarly, Torrini *et al.* demonstrated that depletion of CFL2 in cardiomyocytes augmented F-actin and nuclear YAP (28). In addition, treatment with cytochalasin D, an inhibitor of actin polymerization, prevented the nuclear translocation of YAP, while treatment with jasplakinolide, an actin polymerizer, increased nuclear translocation of YAP (28).

In summary, our study demonstrates that miR-141-3p regulates myogenic differentiation by inhibiting CFL2 expression. We also show that CFL2-YAP-mediated mechanotransduction is a critical component of the myogenic regulation mechanism orchestrated by miR-141-3p. Thus, miR-141-3p may be a critical mediator between mechanotransduction and myogenic differentiation, allowing for the development of an effective target for the diagnosis and therapy in muscle wasting.

4. MATERIALS AND METHODS

4.1. Cell culture

C2C12 cells, a murine myoblast cell line, were cultured in a growth medium (DMEM containing 10% fetal bovine serum and 1% penicillin/streptomycin) and induced myogenic differentiation as previously described (17). Unless otherwise stated, all reagents and materials were purchased from Sigma-Aldrich.

4.2. Cell transfection

CFL2 siRNA (siCFL2), miR-141-3p mimic, antimiR-141 (an inhibitor of miR-141-3p), or scrambled control RNA (scRNA) (Genolution, Seoul, Korea) were transfected into C2C12 myoblasts at 200 nM using Lipofectamine 2000 (Invitrogen). Oligonucleotide sequences are shown in Table S1.

4.3. RNA extraction and Real-Time quantitative PCR

Total RNA from C2C12 cells was extracted using Qiazol (Qiagen) and purified with a miRNeasy Mini Kit (Qiagen). cDNAs were synthesized using a miScript II RT Kit (Qiagen). SYBR Green I (Promega) was used for *q*RT-PCR in a LightCycler 480 (Roche Applied Science). All primer sequences and reaction conditions are shown in Table S2.

4.4. Dual-luciferase reporter assay

Wild-type *CFL2* 3'UTR was synthesized by RT-PCR and inserted into the pmirGLO vector (Promega) using the primer sets described in Table S2. Mutant *CFL2* 3'UTR was generated by site-directed

mutagenesis using the primer set described in Table S2. Dual-luciferase reporter gene assays were performed 24 h after transfection, as described (29).

4.5. Immunoblot analysis

Total protein was extracted using a lysis buffer, which consisted of 2% Triton X-100 and 0.1% phosphatase inhibitor cocktail (Sigma) in PBS, and lysates were dissolved in Laemmli solution (30). For subcellular protein fractionations, the NE-PER nuclear and cytoplasmic extraction reagents (Sigma) were used. Immunoblotting was conducted using specific antibodies described in Table S3. Band intensities were determined by a Fusion Solo (Paris, France).

4.6. Immunofluorescence analysis

After differentiation, C2C12 myoblasts were fixed, permeabilized, and visualized with MyHC antibodies, Alexa 488-conjugated goat anti-mouse antibody (Invitrogen), and Hoechst 33342 (Invitrogen), as described previously (17). Differentiation indices were calculated by expressing numbers of nuclei in MyHC-positive myotubes as percentages of total numbers of nuclei in fields, and fusion indices were calculated by expressing numbers of myotubes with three or more nuclei as percentages of total numbers of nuclei. MyHC-positive areas, numbers of myotubes, and myotube widths were measured using ImageJ Software. All experiments were conducted at least three times using at least five randomly selected fields per experiment.

4.7. F-actin analysis, cell proliferation assays, and flow cytometry analysis

For F-actin staining, cells were fixed, permeabilized, and incubated with FITC-conjugated phalloidin, as described previously (17). Cell proliferation was determined using the Click-iT™ EdU Cell Proliferation Kit (Invitrogen) according to the previous study (17). For flow cytometry analysis, Cell Cycle kit (C03551, Beckman Coulter, USA) was used in a CytoFLEX (Beckman Coulter, USA).

4.8. miRNA target gene predictions and statistical analysis

The potential binding site of miR-141-3p on the *CFL2* 3'UTR was analyzed using publicly available bioinformatics software (TargetScan: www.targetscan.org, miRWalk: mirwalk.umm.uni-heidelberg.de). Results are presented as the means ± standard errors of at least three independent experiments. Statistical significance between groups was determined using the Student's *t*-test.

5. ACKNOWLEDGEMENTS

This study was supported by the National Research Foundation of Korea (NRF) funded by the Korean government (Grant no. NRF-2019R1F1A1040858).

6. CONFLICTS OF INTEREST

The authors have no conflicting interests.

7. FIGURE LEGENDS

Fig. 1. MiR-141-3p repressed CFL2 by binding directly to *CFL2* 3' UTR. (**A**) A potential binding site for miR-141-3p on *CFL2* 3'UTR in various species. (**B**) The wild-type (CFL2-*wt*) and mutant (CFL2-*mut*) binding site on *CFL2* 3'UTR for miR-141-3p. (**C**) A pmirGLO vector containing CFL2-*wt* or CFL2-*mut* was co-transfected with scRNA or miR-141-3p mimic into C2C12 cells, and luciferase activities were analyzed. **(D)** CFL2 protein level was determined 48 h after transfection by immunoblotting. **(E)** CFL2 mRNA level was analyzed 24 h after transfection by RT-PCR (upper) and *q*RT-PCR (lower). All expression levels were normalized to the amount of β-Actin. The values are shown as the relative ratio where the intensity of normalized scRNA control was set to one. Results are presented as means ± SEMs (n>3). *, P<0.05; **, P<0.01; ***, P<0.001 vs scRNA.

Fig. 2. MiR-141-3p increased F-actin formation and nuclear YAP levels. C2C12 myoblasts were transfected with 200 nM of scRNA, siRNA (siCFL2) or miR-141-3p mimic (miR-141-3p). (**A**) After 24 h, CFL2 protein expressions were determined by immunoblotting. (**B**) Representative images of cells stained with FITC-conjugated phalloidin (green) and Hoechst 33342 (blue). Scale bar: 25 μm. (**C**) Immunoblots of YAP and phospho-YAP (pYAP) in the cytoplasm and nuclear fractions. (**D**) Quantitative analysis of immunoblots. The values shown are relative ratios versus scRNA controls. Results are presented as means ± SEMs (n > 3). **, P<0.01; ***, P<0.001 vs scRNA.

Fig. 3. MiR-141-3p promoted myoblast proliferation and cell cycle progression. C2C12 myoblasts were transfected with 200 nM of scRNA, miR-141-3p mimic (miR-141-3p), or antimiR-141. (**A**) Representative images of EdU (green) and Hoechst 33342 (blue) staining. Scale bar: 50 μm. (**B**) Percentages of EdU-positive cells were determined using ImageJ software. (**C**) *q*RT-PCR of PCNA and CCND1. Expression levels were normalized versus U6. (**D**) Flow cytometry after transfection with scRNA or miR-141-3p mimic. Values are presented as relative ratios versus scRNA controls. Results are expressed as means ± SEMs (n > 3). *, P<0.05; **, P<0.01; ***, P<0.001 vs scRNA.

Fig. 4. MiR-141-3p suppressed the expressions of myogenic factors and impaired myogenic differentiation. 200 nM of scRNA control, siCFL2, miR-141-3p mimic (miR-141-3p), or antimiR-141 were transfected into C2C12 cells. (**A**) Immunoblots were obtained after three days of differentiation. (**B**) Quantitative analysis of the protein expressions for CFL2 and myogenic factors. Protein levels were normalized versus β-actin. (**C**) After five days of differentiation, MyHC (green)-positive myotubes were obtained by immunofluorescence staining, and nuclei were counterstained with Hoechst (blue). Scale bar: 50 μm. (**D**), MyHC-positive areas, differentiation indices, fusion indices, and myotube widths were determined as described in the Methods. Results are presented as means ± SEMs (n > 3). ***, P<0.001 vs scRNA.

8. REFERENCES

1. W.R. Frontera, J. Ochala, Skeletal muscle: a brief review of structure and function, Calcif Tissue Int, 96 (2015) 183-195.
2. R. Sartori, V. Romanello, M. Sandri, Mechanisms of muscle atrophy and hypertrophy: implications in health and disease, Nat Commun, 12 (2021) 330.
3. J. Chal, O. Pourquie, Making muscle: skeletal myogenesis in vivo and in vitro, Development, 144 (2017) 2104-2122.
4. G.F. Mok, E. Lozano-Velasco, A. Munsterberg, microRNAs in skeletal muscle development, Semin Cell Dev Biol, 72 (2017) 67-76.
5. J. Krol, I. Loedige, W. Filipowicz, The widespread regulation of microRNA biogenesis, function and decay, Nat Rev Genet, 11 (2010) 597-610.
6. A.J. Sannicandro, A. Soriano-Arroquia, K. Goljanek-Whysall, Micro(RNA)-managing muscle wasting, J Appl Physiol (1985), 127 (2019) 619-632.
7. Y. Gao, B. Feng, S. Han, *et al.*, The Roles of MicroRNA-141 in Human Cancers: From Diagnosis to Treatment, Cell Physiol Biochem, 38 (2016) 427-448.
8. D. Senfter, S. Madlener, G. Krupitza, *et al.*, The microRNA-200 family: still much to discover, Biomol Concepts, 7 (2016) 311-319.
9. B. Fariyike, Q. Singleton, M. Hunter, *et al.*, Role of MicroRNA-141 in the Aging Musculoskeletal System: A Current Overview, Mechanisms of Ageing and Development, 178 (2019) 9-15.
10. G. Zaccagnini, F. Martelli, A. Magenta, *et al.*, p66(ShcA) and oxidative stress modulate myogenic differentiation and skeletal muscle regeneration after hind limb ischemia, J Biol Chem, 282 (2007) 31453-31459.
11. J. Ji, Y. Qin, J. Ren, *et al.*, Mitochondria-related miR-141-3p contributes to mitochondrial dysfunction in HFD-induced obesity by inhibiting PTEN, Sci Rep, 5 (2015) 16262.
12. K.R. Yu, S. Lee, J.W. Jung, *et al.*, MicroRNA-141-3p plays a role in human mesenchymal stem cell aging by directly targeting ZMPSTE24, J Cell Sci, 126 (2013) 5422-5431.
13. S. Periyasamy-Thandavan, J. Burke, B. Mendhe, *et al.*, MicroRNA-141-3p Negatively Modulates SDF-1 Expression in Age-Dependent Pathophysiology of Human and Murine Bone Marrow Stromal Cells, J Gerontol A Biol Sci Med Sci, 74 (2019) 1368-1374.
14. G. Kanellos, M.C. Frame, Cellular functions of the ADF/cofilin family at a glance, J Cell Sci, 129 (2016) 3211-3218.

15. P.B. Agrawal, M. Joshi, T. Savic, *et al.*, Normal myofibrillar development followed by progressive sarcomeric disruption with actin accumulations in a mouse Cfl2 knockout demonstrates requirement of cofilin-2 for muscle maintenance, Hum Mol Genet, 21 (2012) 2341-2356.
16. C.B. Gurniak, F. Chevessier, M. Jokwitz, *et al.*, Severe protein aggregate myopathy in a knockout mouse model points to an essential role of cofilin2 in sarcomeric actin exchange and muscle maintenance, Eur J Cell Biol, 93 (2014) 252-266.
17. M.T. Nguyen, K.H. Min, D. Kim, *et al.*, CFL2 is an essential mediator for myogenic differentiation in C2C12 myoblasts, Biochem Biophys Res Commun, 533 (2020) 710-716.
18. M. Aragona, T. Panciera, A. Manfrin, *et al.*, A mechanical checkpoint controls multicellular growth through YAP/TAZ regulation by actin-processing factors, Cell, 154 (2013) 1047-1059.
19. B.W. Bernstein, J.R. Bamburg, ADF/cofilin: a functional node in cell biology, Trends Cell Biol, 20 (2010) 187-195.
20. S. Dupont, Role of YAP/TAZ in cell-matrix adhesion-mediated signalling and mechanotransduction, Exp Cell Res, 343 (2016) 42-53.
21. Z. Mei, Y. He, J. Feng, *et al.*, MicroRNA-141 promotes the proliferation of non-small cell lung cancer cells by regulating expression of PHLPP1 and PHLPP2, FEBS Lett, 588 (2014) 3055-3061.
22. J.H. Li, Z. Zhang, M.Z. Du, *et al.*, microRNA-141-3p fosters the growth, invasion, and tumorigenesis of cervical cancer cells by targeting FOXA2, Arch Biochem Biophys, 657 (2018) 23-30.
23. D. Guo, H. Jiang, Y. Chen, *et al.*, Elevated microRNA-141-3p in placenta of non-diabetic macrosomia regulate trophoblast proliferation, EBioMedicine, 38 (2018) 154-161.
24. Y. Liu, R. Zhao, H. Wang, *et al.*, miR-141 is involved in BRD7-mediated cell proliferation and tumor formation through suppression of the PTEN/AKT pathway in nasopharyngeal carcinoma, Cell Death Dis, 7 (2016) e2156.
25. W.H. Qian, Y.Y. Liu, X. Li, *et al.*, MicroRNA-141 ameliorates alcoholic hepatitisinduced intestinal injury and intestinal endotoxemia partially via a TLR4-dependent mechanism, Int J Mol Med, 44 (2019) 569-581.
26. L. Zhang, T. Deng, X. Li, *et al.*, microRNA-141 is involved in a nasopharyngeal carcinoma-related genes network, Carcinogenesis, 31 (2010) 559-566.
27. M.G. Mendez, P.A. Janmey, Transcription factor regulation by mechanical stress, Int J Biochem Cell Biol, 44 (2012) 728-732.
28. C. Torrini, R.J. Cubero, E. Dirkx, *et al.*, Common Regulatory Pathways Mediate Activity of MicroRNAs Inducing Cardiomyocyte Proliferation, Cell Rep, 27 (2019) 2759-2771 e2755.
29. W.M. Yang, H.J. Jeong, S.W. Park, *et al.*, Obesity-induced miR-15b is linked causally to the development of insulin resistance through the repression of the insulin receptor in hepatocytes, Mol Nutr Food Res, 59 (2015) 2303-2314.

30. H.S. Ryu, S.Y. Park, D. Ma, *et al.*, The induction of microRNA targeting IRS-1 is involved in the development of insulin resistance under conditions of mitochondrial dysfunction in hepatocytes, PLoS One, 6 (2011) e17343.

Figure 1

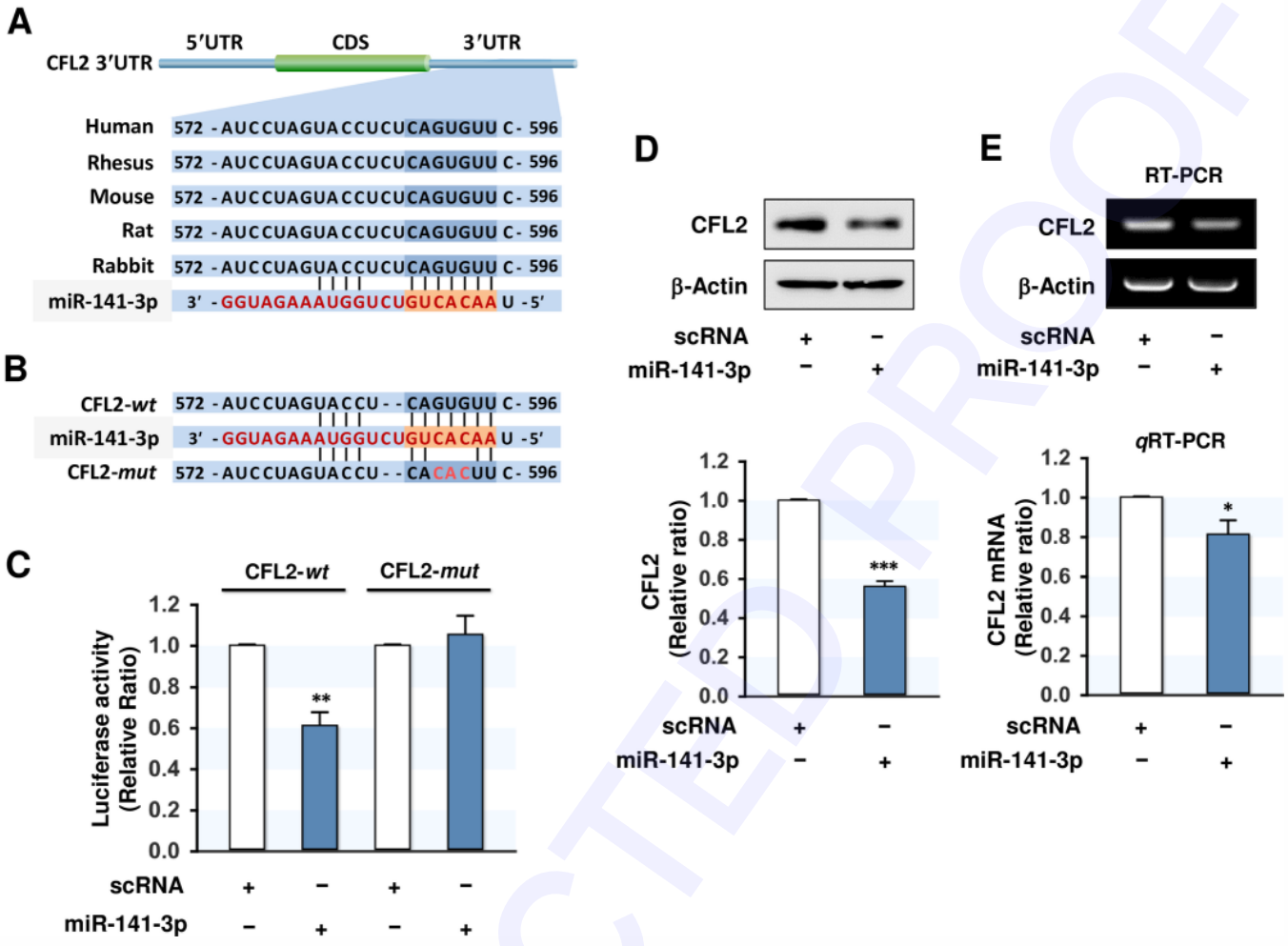

Fig. 1.

Figure 2

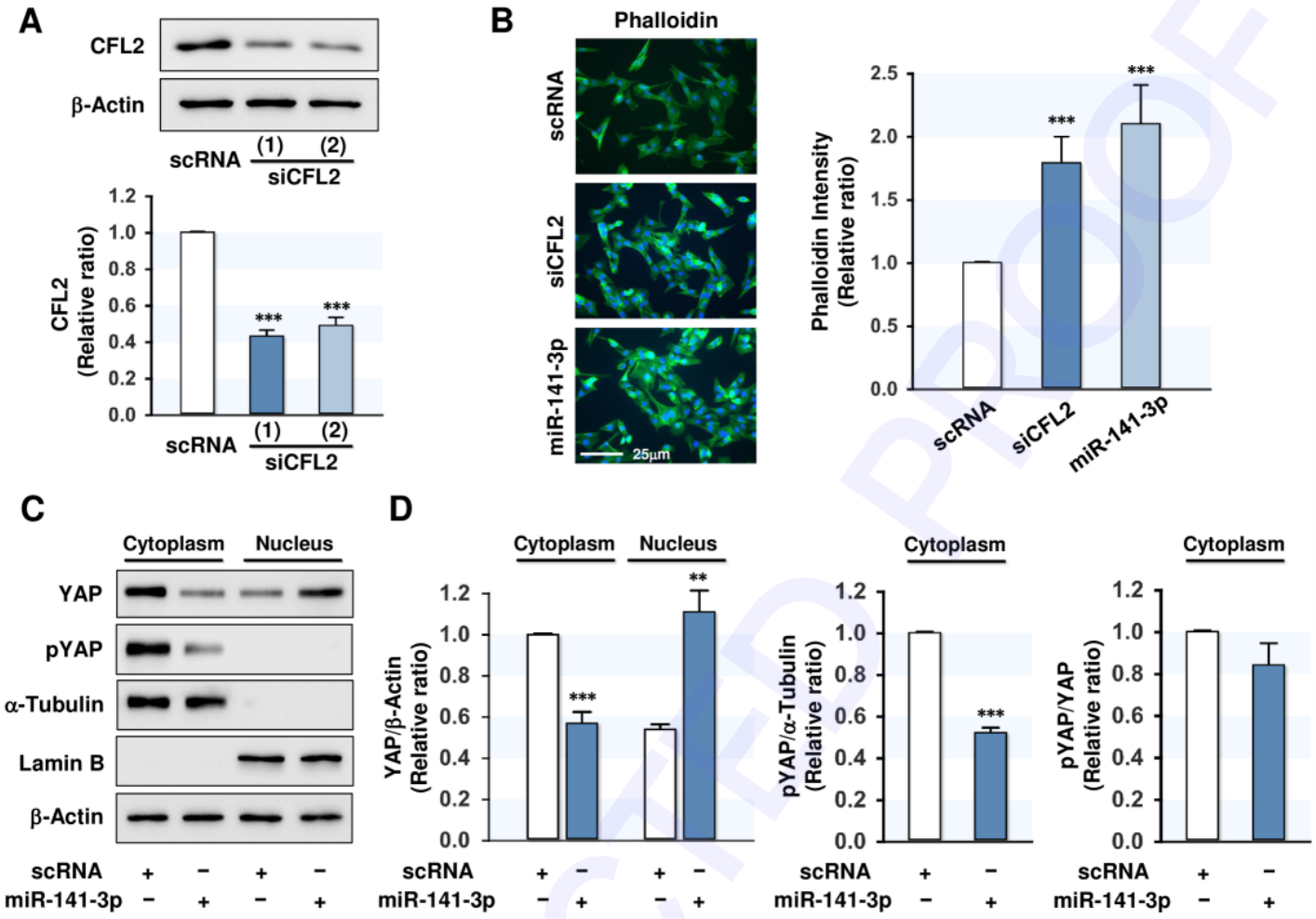

Fig. 2.

Figure 3

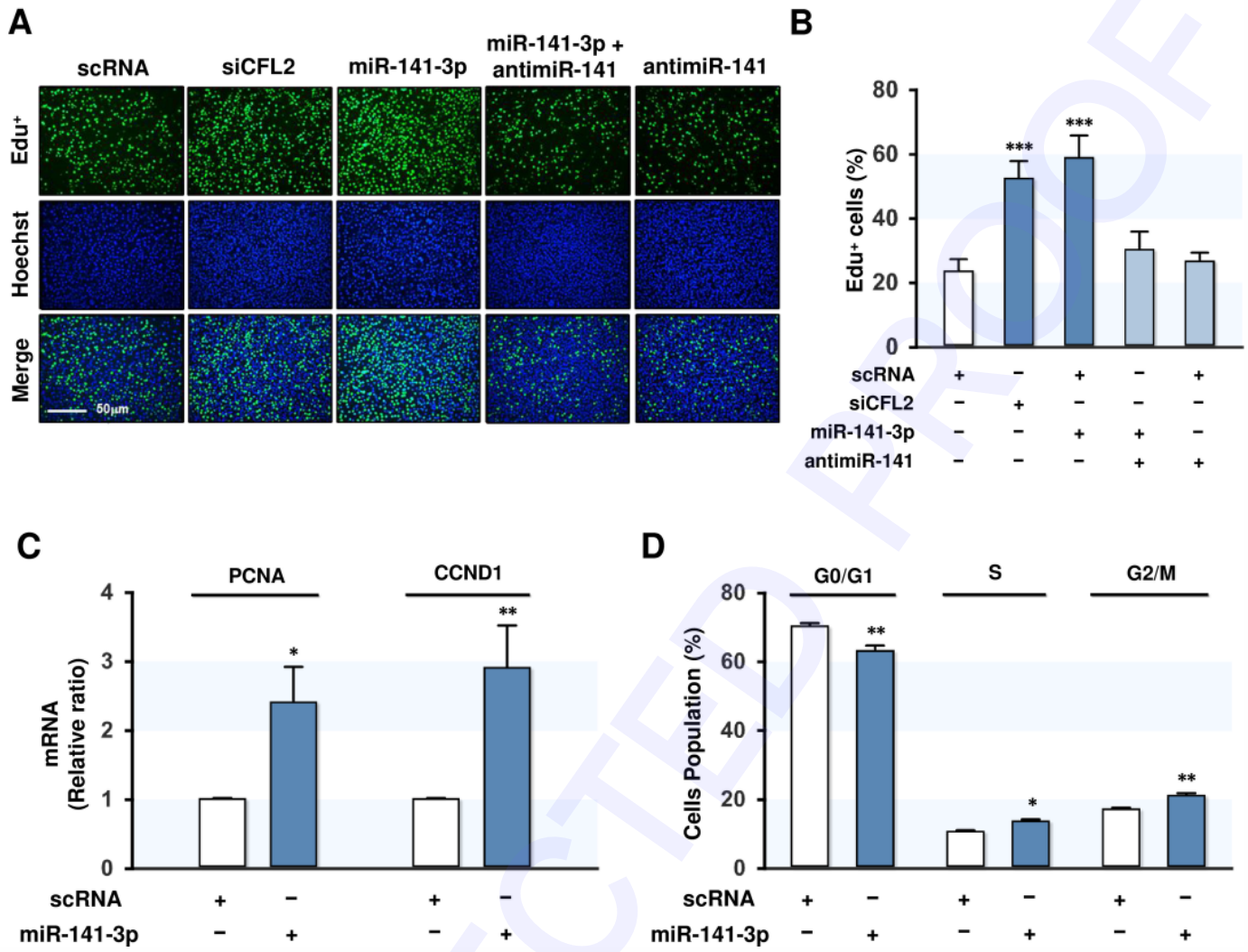

Fig. 3.

Figure 4

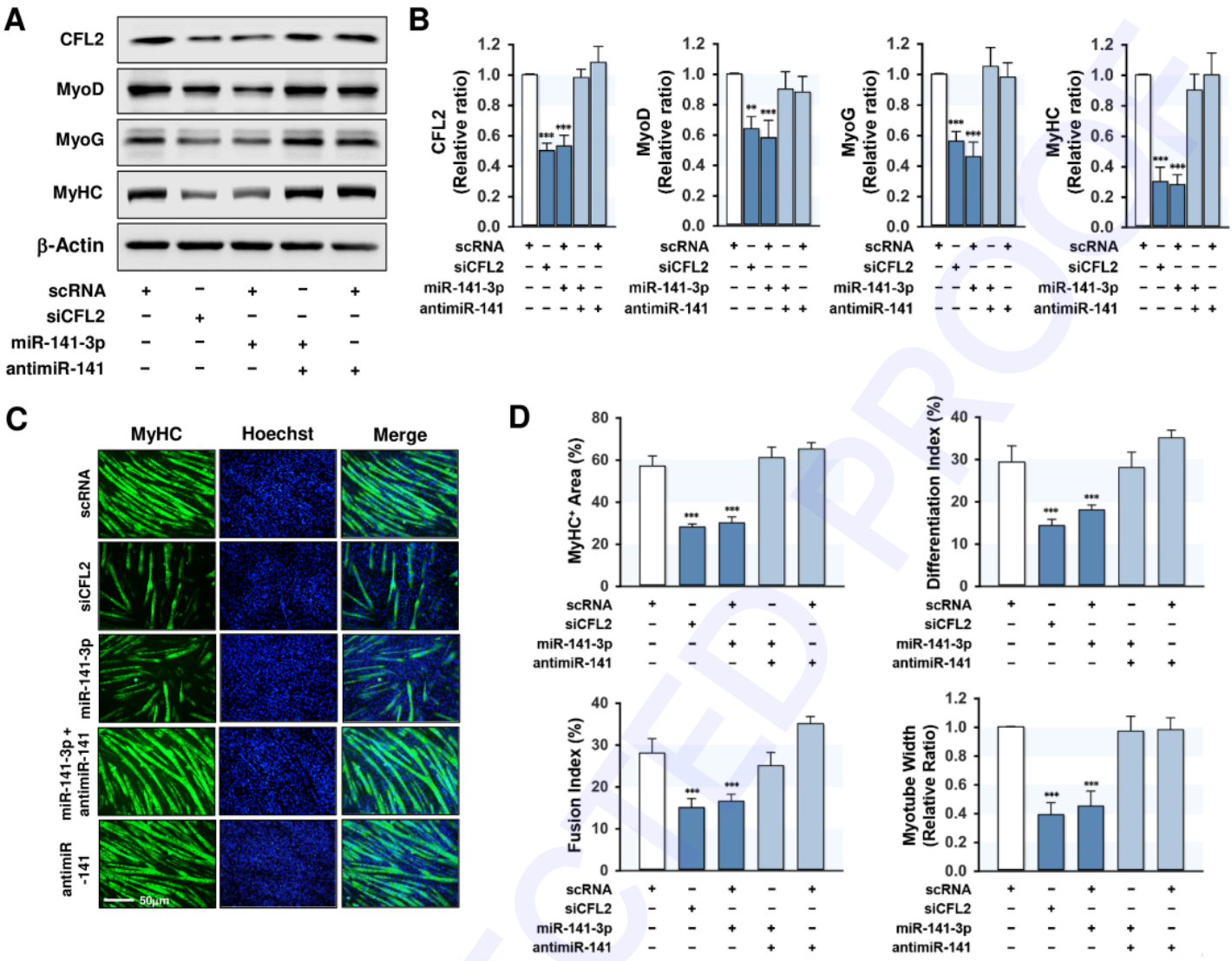

Fig. 4.

Table S1. Oligonucleotide sequences for transfection

Gene	Primer sequence (5´-3´)
scRNA (control RNA)	UGGAAGACUAGUGAUUUUGUUGUU
siCFL2(1)	GCUCUAAAGAUGCCAUUAAUU
siCFL2(2)	CUGAAAGUGCACCGUUAAA
miR-141-3p	UAACACUGUCUGGUAAAGAUGG
antimiR-141	Genolution

Table S2. Primer lists and PCR conditions for *q*RT-PCR, RT-PCR, and cloning

(A) Mouse primer lists for *q*RT-PCR and RT-PCR

Gene		Primer sequence (5´-3´)	Product size	Annealing Temperature	Concentration		Cycle
					cDNA	Primer	
miR-141-3p	F.P	TAACACTGTCTGGTAAAGATGG	90	55	2 ng/μl	0.5 μM	40
	R.P	CCATCTTTACCAGACAGTGTTA					
miRNA universal Primer	R.P	miScript universal primer (Qiagen)					
U6	F.P	CTCGCTTCGGCAGCACA	94				
	R.P	AACGCTTCACGAATTTGCGT					
CFL2	F.P	CCGACCCCTCCTTCTTCTCG	100	58			
	R.P	GTAACTCCAGATGCCATAGTG					
CCND1	F.P	ACCAATCTCCTCAACGACCG	228	58			
	R.P	ACGGAAGGGAAGAGAAGGG					
PCNA	F.P	GAACCTGCAGAGCATGGACTC	201	58			
	R.P	GGTGTCTGCATTATCTTCAGCCC					

(B) Primer lists for cloning of *CFL2* 3´UTR

Gene	Primer sequence (5´-3´)		Product size	Annealing Temperature	Concentration		Cycle
					cDNA	Primer	
CFL2*wt*	F.P	GTATGTGATCGTCAATGTGAATAGC	436	58	2 ng/µl	0.5 µM	35
	R.P	TGCAGGACTCACATGGTAAACAA					
CFL2*mut*	F.P	TCCTAGTACCTCACACTTCATTCC	141				
	R.P	TGCAGGACTCACATGGTAAACAA					
	F.P	GTATGTGATCGTCAATGTGAATAGC	319				
	R.P	GGAATGAAGTGTGAGGTACTAGGA					

Table S3. Antibodies list

Antibody	Type	Host	Manufacturer	Cat. No.	Dilution ratio*
CFL2	Polyclonal	Rabbit	Lifespan Biosciences, Seatlle, WT, USA	LS-C409553	1:2,000
MyHC	Monoclonal	Mouse	DSHB, Iowa,IA, USA	MF20	1:1,000
MyoD	Monoclonal	Mouse	Santa Cruz Biotechnology, Dallas, TX, USA	sc-377460	1:1,000
MyoG	Monoclonal	Mouse	Santa Cruz Biotechnology, Dallas, TX, USA	sc-12732	1:1,000
YAP	Monoclonal	Rabbit	Cell Signaling Technology, Danvers, MA, USA	14074S	1:10,000
p-YAP	Polyclonal	Rabbit	Cell Signaling Technology, Danvers, MA, USA	4911S	1:10,000
Lamin B2	Monoclonal	Rabbit	Abcam, Cambridge, United Kingdom	ab151735	1:2,500
α-Tubulin	Monoclonal	Mouse	DSHB, Iowa,IA, USA	12G10	1:2,000
β-actin	Monoclonal	Rabbit	Sigma-Aldrich Chemical, St. Louis USA	A2066	1:10,000
Antibodies HRP-linked anti-rabbit IgG			Cell Signaling Technology, Danvers, MA, USA	#7074	1:10,000
Goat anti-mouse(H+L)			Invitrogen, Thermofisher Scientific, Waltham, MA USA	#32430	1:2,000

*All blots were visualized using a Femto reagent (Thermofisher Scientific).